Copper indium sulphide nanoparticles with tunable energy band gap obtained by ultrasound-assisted precipitation

A. I. CADIS[a,*], L. E. MURESAN[a], I. PERHAITA[a], L. BARBU-TUDORAN[b,c], G. BORODI[c]
[a]”Raluca Ripan” Institute for Research in Chemistry, “Babes-Bolyai” University, Fântânele 30, 400294 Cluj-Napoca, Romania
[b]Electronic Microscopy Centre, Babes-Bolyai University, Clinicilor 5-7, 400006 Cluj-Napoca, Romania
[c]National Institute for Research and Development of Isotopic and Molecular Technologies, 65-103 Donath, 400293 Cluj-Napoca, Romania

Copper indium sulphide (CIS) nanoparticles were prepared using ultrasound-assisted precipitation, by simultaneous addition of reagents. The Cu-In ratios was varied in order to study its effect on morpho-structural characteristics of CIS. Depending on the composition, the surface area of CIS powders varies between 35.3-114.3 m^2/g and the energy band gap between 1.4-2.9 eV. The morphology, structure and optical properties of the samples were highlighted by UV-Vis spectroscopy, XRD, TEM and BET analysis. The experimental amount of Cu-In ratio was determined based on ICP-OES results and the energy band gap is calculated from UV-Vis spectra using Tauc's relation.

1. Introduction

At present, there has been growing interest for ternary I-III-VI$_2$ semiconductors nanoparticles (NPs) for applications in solar energy harvesting [1,2], light emitting display [3], sensors manufacturing [4], photocatalytic reactions [5] and bio-imaging [6] due to their highly bright luminescence, large absorptivity, tunable properties, large Stokes shift, and relatively good chemical stability, low toxicity and low cost production [7]. As a result, ternary I-III-VI$_2$ semiconductors NPs, such as $CuGaS_2$ [1], $AgInS_2$ [5], $CuInS_2$ [6], $CuInSe_2$ [8], $AgInSe_2$ [8], $CuAlS_2$ [9] or $CuAlSe_2$ [9], have become promising alternatives to II-VI or IV-VI semiconductor NPs that contain toxic elements, such as Cd, Pb, Hg, etc. In addition, the environmental regulations restrict the use of heavy metals in consumers' products [7].

Unlike the more common binary NPs, copper indium sulphide (CIS) NPs, possess unique ternary structures that allow greater structural and compositional flexibility. It has been shown that by varying the molar Cu-In ratios it is possible to control the growth rate with impact on structural and optical properties [10]. Although there is no consensus on the optimal Cu-In precursor ratio, which may differ for different processes, Cu-deficient ratios seem to be preferred [10,11]. Generally, Cu vacancies and In interstitials in CIS compounds are preferred because they produce radiative recombination pathways and improves the NPs optical quality [12].

The CIS NPs are prepared either by solvothermal or hydrothermal routes [13-17]. Some of them use harmful solvents such as N,N-dimethylformamide [15,18]

ethylenediamine [19] and dodecanethiol [20]. In this case, a negative environmental impact is inevitable. The synthesis processes are often placed under harsh conditions (e.g. high vacuum/inert atmosphere and high temperature) requiring sophisticated equipment [15-21]. This undoubtedly increases the cost and energy input, and the production is hardly scaled up to manufacture large amounts of CIS particles on an industrial scale. In this study, we report a facile and low-cost approach to synthesize $Cu_xIn_yS_{0.5x+1.5y}$ NPs with tunable band-gap in water-ethylene glycol solution under mild conditions (e.g. non-vacuum and low temperature) and ultrasounds. Due to its simplicity this synthesis approach has a great potential for industrial applications.

It is known that the solvent used in the precipitation reaction has a strong impact on the characteristics of the final product namely: phase purity, crystallinity, shape and size of particles. In our case, a mixture of water-ethylene glycol was used as solvent in the reaction due to ability to form hydrogen-bonded networks and to have low dielectric constant, low thermal conductivity, and high viscosity. In these conditions, the diffusion rate of ions in the solution is slowed down and therefore the growth of particles is prevented. In addition, ethylene glycol can coordinate the metal ions, consequently, hindering the growth of the particles [22].

Ultrasonic irradiation cause cavitations in a liquid medium, where formation, growth and implosive collapse of bubbles occurred. The collapse of bubbles with short lifetimes produces intense local heating and high pressure. These localized hot spots can generate temperature of

about 5000 °C and pressure of over 1800 kPa appropriate for many chemical reactions [21-24].

In this work, the formation of $Cu_xIn_yS_{0.5x+1.5y}$ NPs is controlled by sonochemical method using a simultaneous addition of reagents with controlled flow, method previously used for synthesis of ZnS [25,26]. The band gap of the $Cu_xIn_yS_{0.5x+1.5y}$ NPs could be tuned by varying the molar ratio of Cu-In precursors. The morphology, porosity, structure and optical properties of the product has been discussed and correlated with composition.

2. Experimental part

2.1. Materials

The preparation of copper indium sulphide powders was performed by ultrasound assisted precipitation, using the reagent simultaneous addition technique (US-SimAdd). The starting reagent were copper (II) chloride dihydrate (≥99.0 %, Sigma-Aldrich), indium (III) chloride, anhydrous (99.99 %, Alfa Aesar), sodium sulphide nonahydrate (98 %, Alfa Aesar), ethylene glycol (p.a., Lach-Ner) and isopropyl alcohol (p.a., S.C. Re Agents Com S.R.L.).

2.2. Samples synthesis

For a typical procedure, equal volumes of aqueous solutions of Cu-In chloride and Na_2S were added into ethylene glycol bottom solution, and kept for maturing. The final ratio water-ethylene glycol is 1:1. The addition of reactants was done under controlled flow (10 mL/min) using an HEIDOLPH 5201 peristaltic pump, at 40 °C, under continuous mechanical stirring and ultrasound in an ELMA Transsonic T660/H bath (35 kHz, at 360 kW output power). The precipitate was allowed to mature for 30 min to complete the reaction, isopropyl alcohol added, separated by centrifugation, washed with isopropyl alcohol and dried at 80 °C for 4 h. In this study were prepared samples with the general formula $Cu_xIn_yS_{0.5x+1.5y}$ were x = 0, 0.05, 0.10, 0.15, 0.20, 0.40, 0.60, 0.80, 1.00 and y = 2-x.

2.3. Characterization of samples

The chemical analysis of CIS powders was carried out by inductively coupled plasma optical emission spectrometry (ICP-OES), using a PERKIN ELMER OPTIMA 2100 DV spectrometer. The copper and indium detection was made at 327.393 nm (detection limit 0.4 µg/L) and 230.606 nm (detection limit 9.0 µg/L), respectively. For ICP-OES analysis, samples were brought in solution by acidic digestion (HCl, HNO_3, HF) using advanced microwave digestion system (MILESTONE - FLEXYWAVE).

The FTIR spectra were carried out with a Thermo Scientific Nicolet 6700 FT-IR spectrometer, using KBr pellet technique and UV-Vis spectra were carried out with a JASCO-V650 spectrophotometer with an integration sphere (ILV-724).

Specific surface area and porosity measurements were made on decontaminated samples of any traces of moisture or other adsorbents, using a Micromeritics, TriStar II 3020 - Surface Area and Porosity Analyzer. Adsorption-desorption isotherms were measured close to the boiling point of nitrogen (77 K). Gas pressure was gradually increased to the saturation value, when condensation of the adsorbate (N_2) occurs into the powder pores.

Structure and microcrystalline parameters were evaluated based on X-ray diffraction (XRD) performed using a 600 Shimadzu diffractometer at 40 kV and 40 mA using Cu kα1 radiation (1.54056 Å) in the 2θ range 10 - 80°.

The size and morphology of the samples were revealed by transmission electron microscopy (TEM) using a Hitachi HD 2700 electron microscope.

3. Results and discussion

3.1. General characterization

The ICP-OES analysis was performed in order to determine the experimental concentrations of Cu and In ions from CIS powders. The Cu co-precipitation level was estimated based on the ratio between the experimental and the theoretic copper concentration. The results are shown in table 1. It can be seen that the experimental concentration of copper is slowly higher than theoretical values for all samples excepting sample with 2.5 % Cu.

Table 1. The ICP-OES analysis data for CIS powders obtained with different reactants concentrations

Nr. Crt.	$Cu_{theo.}$ (%mol)	$Cu_{exp.}$ (%mol)	$In_{theo.}$ (%mol)	$In_{exp.}$ (%mol)	$Cu_{exp.}/Cu_{theo.}$ (%mol)	Theoretic formula	Experimental formula
1	0	0	100.0	100.0	-	In_2S_3	In_2S_3
2	2.5	2.2	97.5	97.8	87.4	$Cu_{0.05}In_{1.95}S_{2.95}$	$Cu_{0.04}In_{y1.96}S_{2.96}$
3	5.0	5.1	95.0	94.9	101.1	$Cu_{0.10}In_{1.90}S_{2.90}$	$Cu_{0.10}In_{1.90}S_{2.90}$
4	7.5	7.6	92.5	92.4	101.1	$Cu_{0.15}In_{1.85}S_{2.85}$	$Cu_{0.15}In_{1.85}S_{2.85}$
5	10.0	10.5	90.0	89.5	104.5	$Cu_{0.20}In_{1.80}S_{2.80}$	$Cu_{0.21}In_{1.79}S_{2.79}$
6	20.0	21.0	80.0	79.0	104.9	$Cu_{0.40}In_{1.60}S_{2.60}$	$Cu_{0.42}In_{1.58}S_{2.58}$
7	30.0	32.1	70.0	67.9	107.1	$Cu_{0.60}In_{1.40}S_{2.40}$	$Cu_{0.64}In_{1.36}S_{2.36}$
8	40.0	40.6	60.0	59.4	101.5	$Cu_{0.80}In_{1.20}S_{2.20}$	$Cu_{0.81}In_{1.19}S_{2.19}$
9	50.0	52.0	50.0	48.0	104.1	$Cu_{1.00}In_{1.00}S_{2.00}$	$Cu_{1.04}In_{0.96}S_{1.96}$

FTIR spectra of CIS samples were recorded in the range of 400–4000 cm^{-1} in order to gather information on the presence of functional groups. In figure 1 are shows the FTIR spectra of CIS samples in comparison with FTIR spectra of ethylene glycol. The EG spectrum show the characteristic absorption bands of ν_{O-H} (3372 cm^{-1}), $\nu_{as\ C-H}$ (2947 cm^{-1}), $\nu_{s\ C-H}$ (2880 cm^{-1}), δ_{O-H} (1656 cm^{-1}), δ_{C-H} (1460 cm^{-1}), ν_{C-O-H} (1086 cm^{-1}), ν_{C-O-C} (1043 cm^{-1}), γ_{C-H} (885 cm^{-1}), ν_{C-C} (863 cm^{-1}) and δ_{C-O} (522 cm^{-1}). Some of them are visible along with the bands of In–S bond (~620 cm^{-1}) and Cu-S (~532 cm^{-1}). The stretching and bending absorption bands of water (3390 cm^{-1} and 1654 cm^{-1}) and EG oxidation products (ex. diacetyl, $\nu_{C=O}$ at 1620 cm^{-1}) [27,28] are also observed.

FT-IR investigations put in evidence the high capacity of CIS powders to absorb organic compounds from the precipitation medium, thus illustrating their large surface area in correlation with the small particle dimensions.
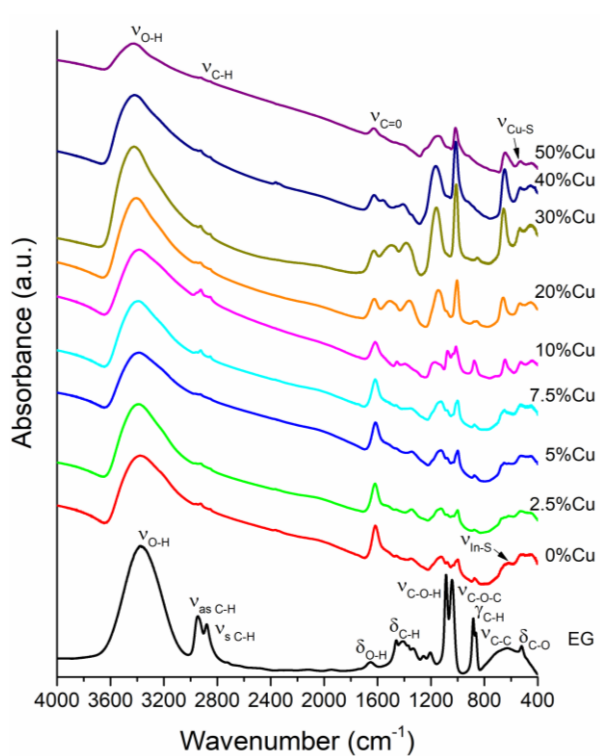
Fig. 1. FTIR spectra of ethylene glycol (EG) and CIS samples prepared with different Cu-In ratio (color online)

3.2. Optical characterization

Fig. 2a presents the UV−Vis absorption spectra of CIS powders with different concentration of Cu ions. The samples show a gradual red shift with increasing of Cu amount indicating a decrease in optical band gap. Undoped In$_2$S$_3$ presents an absorption band with maxima at 354 nm. When doped with 2.5 % Cu the spectrum is changed by apparition of a second absorption band with maximum at ≈ 409 nm. The continuous increase of Cu amount up to 50 % broadens the absorption band,

increases the intensity and shifts it towards higher wavelengths (463 nm).
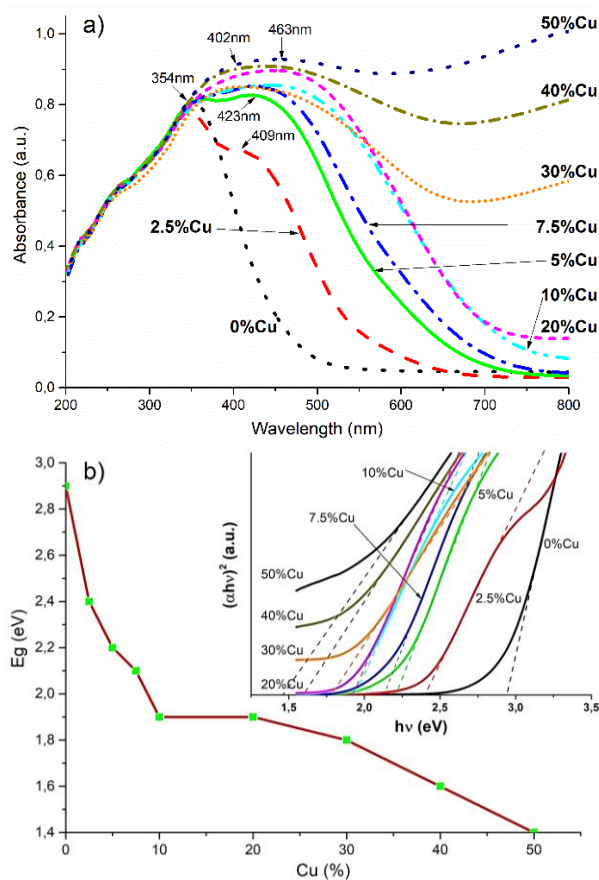
Fig. 2. UV-Vis spectra of CIS samples (a) and bandgap vs. Cu concentration (b). The Tauc plots is shown in the insert of (b) (color online)

The energy band gap of the CIS samples can be estimated using Tauc's relation:

$$(\alpha h\upsilon)^n = k(h\upsilon - E_g)$$

where E$_g$ is the band gap energy (eV), h is the Planck's constant, α is the absorption coefficient, ν is the light frequency and n is 2 for a direct band gap semiconductor.

Fig. 2b presents the variation of band gap with Cu concentration calculated with Tauc's relation (showed in insert of Fig. 2b). The band gap decrease with the increase of copper content from 2.9 eV (0 % Cu) to 1.4 eV (50 % Cu). The results suggest that a tunable band gap could be achieved through adjusting the Cu amount.

3.3. Morpho-structural characterization

Surface area and porosity measurements were performed in order to illustrate the changes of the CIS powder surface states.

Fig. 3a shows adsorption/desorption isotherms for two representative samples, namely sample with 2.5 % Cu and 10 % Cu.

All samples present similar isotherms, type IV, characteristic for mesoporous material. Excepting sample with 2,5% Cu, the hysteresis loops were identified to be type H2, which indicate the presence of interconnected pores with different shapes and sizes. In case of sample with 2.5 % Cu the hysteresis is H1 type and corresponding to uniform elongated pores [29, 30].
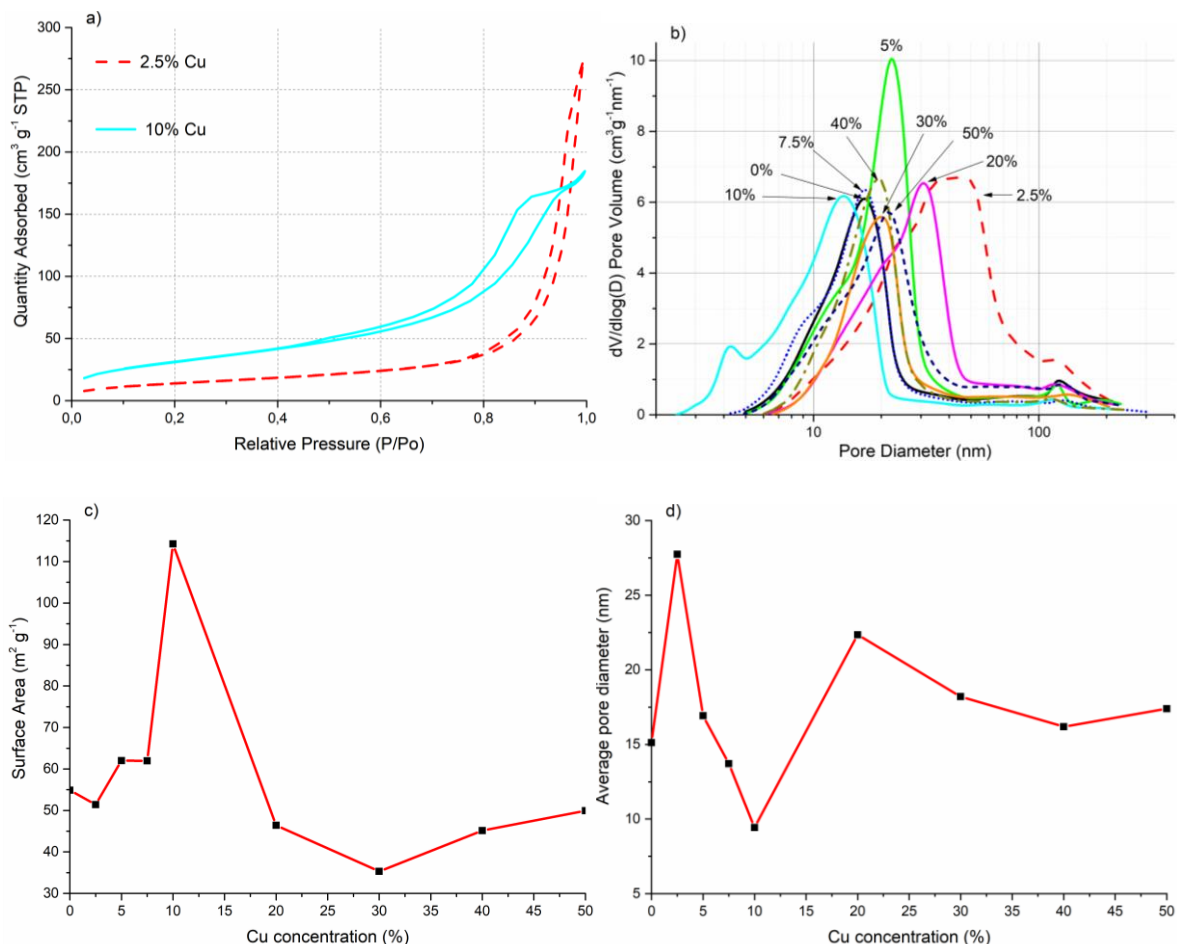
Fig. 3. Adsorption–desorption isotherms (a). Pore volume distribution curves (b). Effect of synthesis conditions on surface area (c) and pore size (d) of CIS samples (color online)

JH (Baret, Joyner and Halenda method) analysis was used to determine area and volume of the meso-pores using adsorption and desorption techniques. Figure 3b shows the pore volume distributions in 2-400 nm range. All samples show a multimodal distribution curve in the meso-porous domain with pore diameter situated between 13 nm and 45 nm, indicating heterogeneous powders. The quantity of adsorbed nitrogen depends on Cu amount. For example, sample with 2.5 % Cu absorbs the highest quantity of nitrogen among the samples which is confirmed by the highest pore volume (0.44 cm^3/g) and the highest average pore diameter (27.7 nm) meaning that this sample is the most porous. On the other hand, sample with 10 % Cu present a lower pore volume (0.31 cm^3/g) with

the pore diameter of 9.4 nm. The sample with the highest copper content (50 %) presents a pore volume of 0.28cm^3/g with an average pore diameter of 17.4 nm.

Fig. 3c and 3d illustrates the dependence of surface area and average pore diameter on the copper concentration. The specific surface area of sample varies with the copper content: 51.4 m^2/g (2.5 % Cu); 114.3 m^2/g (10% Cu); 46.41 m^2/g (20% Cu) and 49.92m^2/g (50% Cu).

The TEM micrographs of samples with 0 % Cu and 50 % Cu (Fig. 4 a,b) are very similar. It was found that CIS nanoparticles are spherical with diameters up to 15 nm that tends to agglomerate due to the high surface making difficult to identify of a single particle.
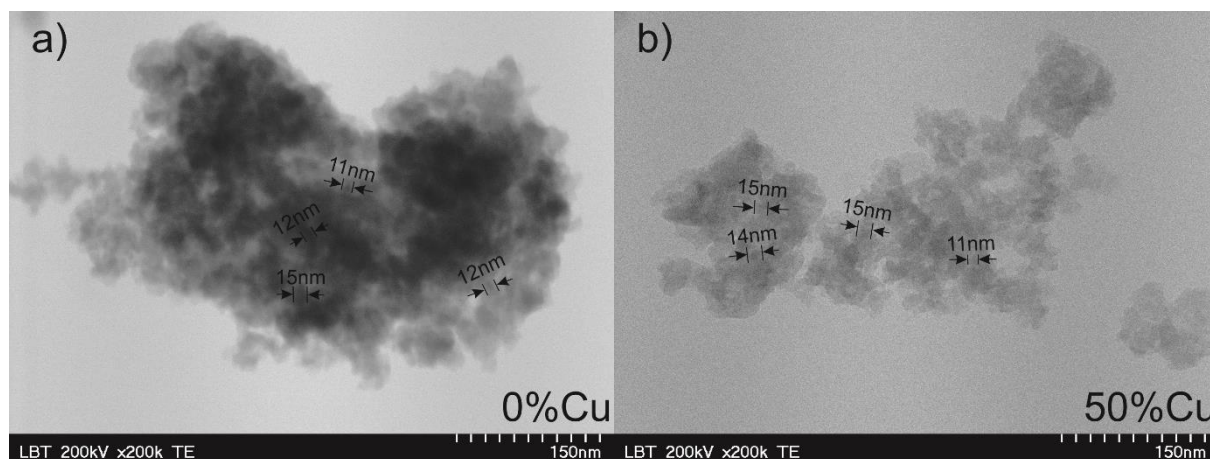
Fig. 4. TEM images of two of CIS samples. (a) sample with 0 % Cu; (b) sample with 50 % Cu

The XRD patterns of CIS samples are shown in Fig. 5. From the broadening of the diffraction lines, it can be established that synthesized particles are nanocrystalline. The XRD presents two major diffraction bands at 28° and 48° indexed to standard In_2S_3 (ICSD 64-0361). By substitution of In^{3+} with Cu^+ the two diffraction bands move slightly to larger angles, due to differences in ion size ($r_{In3+} = 76$ pm and $r_{Cu+} = 74$ pm).

Over 20 % Cu doping level it can be observed that the diffractograms presents along with the broad peaks of CIS several narrow lines identified to be from crystalline sulphur (S_8) (PDF 08-0247).
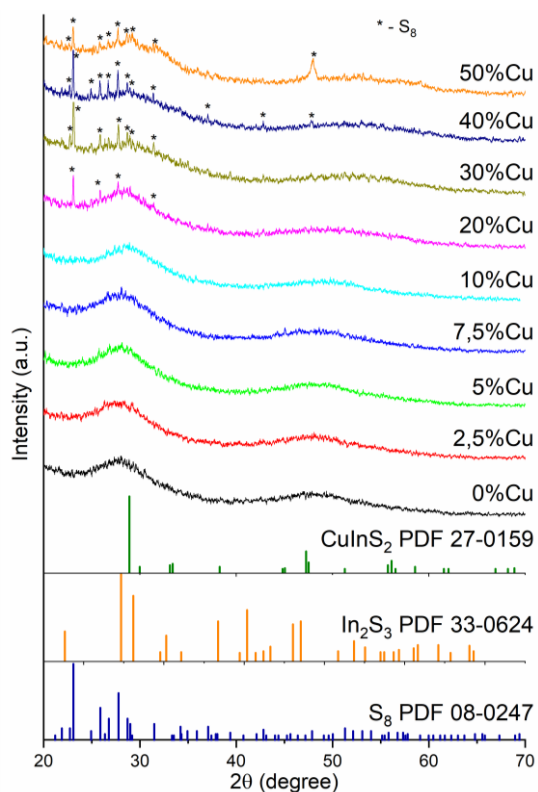
Fig. 5. XRD patterns of CIS samples prepared with different Cu In ratio (color online)

The XRD data's were used to determine the crystallite size of the synthesized CIS samples. For this, the Scherrer's formula was used to calculate the grain size of the particles.

$$D = \frac{k\lambda}{\beta cos\theta}$$

where, D is the crystallite size (Å), k=0.9 is the Scherrer's constant, λ is the X-ray wavelength (Cu $K_\alpha = 1.5405$ Å), β is the full width at half maximum (FWHM in radians), θ is the Bragg's angle in degrees. The calculated crystallite sizes of CIS nanopowders increase from 1,60 nm (0 % Cu) to 2,05 nm (7.5 % Cu) and, after that, decreases to 1,48 nm (50 % Cu). It is worth noting that the Debye-Scherrer equation for calculating crystallite size makes sense to use in a few special cases. The value of the constant in the above equation accounts for the shape of the particle. It does not take into consideration the presence of a size distribution or the existence of intrinsic point defects formed in the lattice. Hence, diameter of the crystallite from FWHM of the peak can overestimate the experimental value as the larger crystallite contribute more to the diffraction pattern than smaller crystallite in terms of intensity.

4. Conclusions

CIS nanocrystalline powders were prepared by ultrasound-assisted precipitation, using simultaneous addition of reagents. The CIS powders consist on rounded particles of about 15 nm kept together in agglomerates. The pore diameters are situated in meso-domain and the specific surface range from 35.3 m^2/g (30 % Cu) to 114.3 m^2/g (10 % Cu). The crystallite sizes vary between 1,4 nm (50 % Cu) and 2.0 (7.5 % Cu). The Cu and In amounts confirmed by ICP-OES measurements are closed to theoretical values. The energy band gap of powders determined from UV-Vis spectra can be tuned by controlling Cu-In ratio from 2.9 eV (0 % Cu) to 1.4 eV (50% Cu).

Acknowledgments

The authors are grateful to the Babes Bolyai University for financial support.

References

[1] M. Jalalah, M. S. Al-Assiri, J. G. Park, Adv. Energy Mater. **8**(20), 1703418 (2018).

[2] J. Zhao, T. Minegishi, G. J. Ma, M. Zhong, T. Hisatomi, M. Katayama, T. Yamada, K. Domen, Sustain. Ener. Fuels **4**(4), 1607 (2020).

[3] D. V. Talapin, J. S. Lee, M. V. Kovalenko, E. V. Shevchenko, Chem. Rev. **110**(1), 389 (2009).

[4] M. Mou, Y. Wu, H. Zou, J. Dong, S. Wu, Z. Yan, S. Liao, Sens. Actuator B: Chem. **284**, 265 (2019).

[5] F. Deng, F. Zhong, D. Lin, L. Zhao, Y. Liu, J. Huang, X. Luo, S. Luo, D. D. Dionysiou, Appl. Catal. B: Environ. **219**, 163 (2017).

[6] T. Pons, E. Pic, N. Lequeux, E. Cassette, L. Bezdetnaya, F. Guillemin, F. Marchal, B. Dubertret ACS Nano **4**(5), 2531 (2010).

[7] J. Kolny-Olesiak, H. Weller, ACS Appl. Mater. Interfaces **5**(23), 12221 (2013).

[8] S. Ghoshal, L. B. Kumbhare, V. K. Jain, G. K. Dey, Bull. Mater. Sci. **30**(2), 173 (2007).

[9] S. Sugan, K. Baskar, R. Dhanasekaran, J. Alloy. Compd. **645**, 85 (2015).

[10] B. T. Zhang, Y. C. Wang, C. B. Yang, S. Y. Hu, Y. Gao, Y. P. Zhang, Y. Wang, H. V. Demir, L. W. Liu, K. T. Yong, Phys. Chem. Chem. Phys. **17**(38), 25133 (2015).

[11] R. L. Zhang, P. Yang, Y. Q. Wang, J. Nanopart. Res. **15**(9), 1 (2013).

[12] S. C. Shei, W. J. Chiang, S. J. Chang, Nanoscale Res. Lett. **10**, 122 (2015).

[13] N. Chumha, W. Pudkon, A. Chachvalvutikul, T. Luangwanta, C. Randorn, B. Inceesungvorn, A. Ngamjarurojana, S. Kaowphong, Mater. Res. Express **7**(1), 015074 (2020).

[14] N. Chumha, T. Thongtem, S. Thongtem, D. Tantraviwat, S. Kittiwachana, S. Kaowphong, Ceram. Int. **42**(14), 15643 (2016).

[15] J. Benbelgacem, A. Ben Marai, R. Mendil, K. Medjnoun, K. Djessas, Z. Ben Ayadi, J. Alloys. Compd. **692**, 966 (2017).

[16] M. H. Chiang, W. T. Lin, B. S. Wang, K. C. Hsu, Y. S. Fu, Ceram. Int. **43**(7), 5819 (2017).

[17] D. Pan, L. An, Z. Sun, W. Hou, Y. Yang, Z. Yang, Y. Lu, J. Am. Chem. Soc. **130**(17), 5620 (2008).

[18] X. Lu, F. Deng, M. Liu, X. Luo, A. Wang, Mater. Chem. Phys. **212**, 372 (2018).

[19] P. Bera, S. I. Seok, J. Solid State Chem. **183**(8), 1872 (2010).

[20] W. S. Song, H. Yang, J. Nanosci. Nanotechnol. **13**(9), 6459 (2013).

[21] O. Amiri, M. Salavati-Niasari, M. Mousavi-Kamazani, D. Ghanbari, M. Sabet, K. Saberyan, Bull. Mater. Sci. **37**(5), 1079 (2014).

[22] S. Kaowphonga, N. Chumha, Russ. J. Inorg. Chem. **64**(11), 1469 (2019).

[23] A. R. Tomsa, E. J. Popovici, A. I. Cadis, M. Stefan, L. Barbu-Tudoran, S. Astilean, J. Optoelectron Adv. M. **10**(9), 2342 (2008).

[24] M. Salavati-Niasari, G. Hosseinzadeh, F. Davar, J. Alloys. Compd. **509**(1), 134 (2011).

[25] A. I. Cadis, L. E. Muresan, I. Perhaita, V. Munteanu, Y. Karabulut, J. Garcia Guinea, A. Canimoglu, M. Ayvacikli, N. Can, Opt. Mater. **72**, 533 (2017).

[26] A. I. Cadis, I. Perhaita, V. Munteanu, L. Barbu-Tudoran, D. T. Silipas, L. E. Muresan, Colloid. Polym. Sci. **295**(12), 2337 (2017).

[27] K. Krishnan, R. S. Krishnan, Proc. Indian Acad. Sci. A **64**, 111 (1966).

[28] N. Chumha, T. Thongtem, S. Thongtem, S. Kittiwachana, S. Kaowphong, J. Ceram. Process. Res. **18**(12), 871 (2017).

[29] K. S. W. Sing, D. H. Everett, R. A. W. Haul, L. Moscou, R. A. Pierotti, J. Rouquerol, T. Siemieniewska, Pure Appl. Chem. **57**(4), 603 (1985).

[30] P. A. Webb, C. Orr, Analytical methods in fine particle technology, Micromeritics Instrument Corporation Publishers, Norcross, USA, 161 (1997).

---

*Corresponding author: adrian_cadis@yahoo.ro